Vietnam Journal of Science and Technology ***63*** *(4) (2025) 768-779*

doi:10.15625/2525-2518/19437

Optimizing the preparation of nanoemulsions based on sacha inchi (*Plukentia volubilis* L.) seed oil by response surface methodology

Dam Xuan Thang[1], Cung Dinh Duc[1], Nguyen Ngoc Quynh[1], Pham Thi Tham[1], Thai Hoang[2, 3], Nguyen Phi Hung[4], Nguyen Thuy Chinh[2, 3, *]

[1]*Hanoi University of Industry, 298 Cau Dien, Bac Tu Liem, Ha Noi, Viet Nam*

[2]*Institute for Tropical Technology, Vietnam Academy of Science and Technology, 18 Hoang Quoc Viet, Cau Giay, Ha Noi, Viet Nam*

[3]*Graduate University of Science and Technology, Vietnam Academy of Science and Technology, 18 Hoang Quoc Viet, Cau Giay, Ha Noi, Viet Nam*

[4]*Institute of Natural Products Chemistry, Vietnam Academy of Science and Technology, 18 Hoang Quoc Viet, Cau Giay, Ha Noi, Viet Nam*

[*]Email: *thuychinhhn@gmail.com* or *ntchinh@itt.vast.vn*

Received: 17 November 2023; Accepted for publication: 28 October 2024

Abstract. This work presents the use of Sacha Inchi (*Plukentia volubilis* L.) seed oil (SO) as an oily phase for preparing nanoemulsion systems. The pseudo-ternary phase diagram for SO, water, and surfactants has been constructed to find the suitable range for components of the emulsion systems. The optimization has been processed to investigate the optimal composition of components of the emulsion systems. Three technology factors including SO volume, Tween 80 volume, and distilled water volume with low level (-1) and high level (+1) have been selected while the droplet size was used as an objective function. The optimization was carried out using response surface methodology (RSM) and Box-Behnken design (BBD). The results showed a high fitting of the theoretical model and experimental data. The optimal conditions were found at SO of 266 µL, Tween 80 of 264 µL, and distilled water of 483 µL. Under the optimal conditions, the droplet size of the nanoemulsion was 57.9 ± 1.5 nm. Other characteristics of the nanoemulsion prepared under the optimal conditions have been evaluated by using infrared (IR) spectroscopy, stereo microscopy (SM), zeta potential, and ultraviolet-visible (UV-Vis) spectroscopy.

Keywords: nanoemulsion, Sacha Inchi (*Plukentia volubilis* L.) seed oil, surfactant, droplet size, response surface methodology.

Classification numbers: 2.4.3, 2.7.1.

1. INTRODUCTION

In recent years, Sacha Inchi (*Plukentia volubilis* L., or Sachi) seed has been considered an excellent source of bioactive substances, in particular, very high content of polyunsaturated fatty

acids, sterols, and tocopherols [1-5]. In a report, the fatty acids and their corresponding content (% of total fatty acids) in Sachi seed are: palmitic (C16:0) 1.6 - 2.1 %; stearic (C18:0) 1.1 - 1.3 %; oleic (C18:1, ω-9) 3.5 - 4.7 %; linoleic (C18:2, ω-6) 12.4 - 34.98 %; and α-linoleic acid (C18:3, ω-3) 12.8 - 47.04 %. Total saturated fatty acids (SFAs) are 2.6 - 3.2 % and total unsaturated fatty acids (UFAs) are 30.6-34.3 %. When converted to oil, the content of palmitic, stearic, oleic, linoleic an,d α-linolenic acid are 4.7 ± 0.2, 3.3 ± 0.1, 8.9 ± 0.1, 34.1 ± 0.1, and 48.2 ± 0.4, respectively [1]. In other reports, Sachi seed consists of oil (35 - 60 %), protein (25 - 30 %) (including leucine, isoleucine, tyrosine, tryptophan, and lysine), vitamin E, polyphenols, tannins, carotenoids, saponins, lectins, alkaloids, and minerals [3, 4]. The Sachi seed oil contains a high content of essential fatty acids (ω-6, ω-3), in which, linoleic occupied 34 - 37 % and linolenic occupied 42 - 51 % in 90 % of the total fatty acids. Thanks to a high content of essential fatty acids, safety, and odorless, Sachi seed oil is a valuable ingredient in food applications. Similarly to Sachi seed oil in other countries, the Sachi seed oil extracted from plants growing in Viet Nam had a high fatty acids content, for example, linoleic (42.62 %), linolenic (36.32 %), and oleic (11.64 %) [6]. Due to its valuable bioactivity, Sachi seed oil is very potential to act as an oily phase in microemulsion systems for applications in the pharmaceutical field, cosmetic and personal hygiene products.

Xiaoqiu Song *et al.* studied the preparation of Sachi oil microemulsion systems [7]. The pseudo-ternary phase diagrams have been constructed using the water titration method to evaluate the effect of non-ionic surfactants, essential oils, short-chain alcohols, and straight-chain esters. The authors found that Tween 80 surfactant can well solubilize the maximum oil and induce the formation of microemulsions [7].

The type and ratio of oily phase, water phase, and surfactant have a strong effect on the size and stability of the emulsion system [8 - 10]. A nanoemulsion is often used to enhance the delivery of bioactive pharmaceutical ingredients while a microemulsion is usually manufactured to deliver vaccines or kill microbes [11 - 13]. The particle size of nanoemulsions ranged from 20 nm to 200 nm. These systems have a high kinetic stability but a low thermal stability [11]. To prepare the nanoemulsions, a mechanical shear, for example, ultrasonication, has been requested to obtain smaller droplets [12].

Sachi oil has a hydrophilic-lipophilic balance (HLB) value of 8.5 [14], so, it is suitable to play the role of oily phase in emulsion systems. Although Sachi seed oil has been used as an oily phase in microemulsion systems, the optimization of Sachi seed oil, water, and surfactant composition for the preparation of a nanoemulsion has still been limited in research. Therefore, the aim of this study is to optimize the components of a nanoemulsion formed from sachi seed oil, distilled water, and surfactant. A nanoemulsion oil in water (O/W) is composed of a Sachi seed oil phase dispersed in an aqueous. Tween 80 with a HLB of 15, within the range of HLB 8 - 18 for O/W emulsifiers. The effectiveness of Sachi seed oil emulsion has also been proved [7], thus, it will be used in this study as a surfactant. The optimization was processed using the Box-Behnken design type by response surface methodology (RSM). In addition, some characteristics of the nanoemulsion at the optimal conditions will be assessed by infrared (IR), stereo microscopy (SM), size distribution, Zeta potential, and ultraviolet-visible (UV-Vis) methods.

2. MATERIALS AND METHODS

2.1. Materials

Sachi seed oil (SO, Viet Nam) with omega-3, omega-6, and omega-9 content of 45 %, Tween 80 (polysorbate 80, China) with a fatty acid content of ≥ 58 %, and distilled water (99.9 %, Viet Nam) were used as received.

2.2. Setting up the phase diagram

The procedure for setting up the pseudo-ternary phase diagram for three components, consisting of SO, Tween 80 surfactant, and distilled water was as follows. Firstly, nine clean, dry, and marked bottoms were prepared before adding 20 - 180 µL of SO into them with an increased volume step of 20 µL. Next, 180 - 20 µL of Tween 80 surfactant was added to these bottoms with a decreased volume step of 20 µL. The mixtures were vortexed to reach a homogeneity. Then, the distilled water was added to these bottoms and the mixture was vortexed. The water-adding process will be stopped when the mixture is transferred to turbidity. The pseudo-ternary phase diagram for three components was set up on TriDraw2.6 software.

2.3. Preparation of nanoemulsion

To prepare the nanoemulsion, SO and surfactant were mixed and vortexed for 5 minutes before adding distilled water. Next, the mixture was vortexed for 5 minutes following ultrasonicating on a Q500 Sonicator for 30 minutes at 40 ^{o}C. After ultrasonicating, the mixture was vortexed for 5 minutes and stored in a fridge for 24 hours to stabilize the nanoemulsion system.

2.4. Experimental design for optimization

In this study, three technology factors consist of SO volume, Tween 80 volume, and distilled water volume with low level (-1) and high level (+1) as presented in Table 1.

Table 1. Experimental levels of technological variables.

Real variable	Encoding variable	Variation (Δ)	Research level		
			-1	0	+1
Sachi seed oil (µL)	A	50	200	250	300
Tween 80 (µL)	B	100	200	300	400
Distilled water (µL)	C	50	450	500	550

These factors (SO volume, Tween 80 volume, and distilled water volume) correspond to three variables, A, B, and C, respectively. The objective function is the droplet size. To give the range of ending code, we based on the data of the ternary phase diagram, some results from the initial survey experiments as well as referred from other related reports about similar objectives [8, 9]. In this study, the concentration of Tween 80 has been chosen from 200 - 400 µL, corresponding to 23.53 - 32.00 %, lower than the concentration of mixture surfactants (from 55.00 to 65.00 %) in the turmeric oil/water emulsion as reported by Suraj *et al.* [8]. This may be the difference in the nature of SO and turmeric oil. The combination of SO and water to form an emulsion requires a lower surfactant concentration. The aim of optimization is to minimize the size of droplets in nanoemulsion systems. The experiments were conducted with fifteen samples that were designed according to BBD by using Design Expert 23.1.0 software (Stat-Ease, Inc.). A central point was evaluated three times to ensure precision and reliability. A quadratic model and analysis of variance (ANOVA) statistical model have been calculated to evaluate the fitting of theory and experiment. The experiment was designed according to the Box-Behnken type and optimized by response surface methodology (RSM).

2.1. Characterization

Infrared (IR) spectrum of the nanoemulsion prepared under the optimal condition was recorded by an IR spectrometer (Nicolet iS10, USA). The morphology of the nanoemulsion was evaluated by stereo microscopy (SM) method using the Olympus device (SZ61, Japan). The size distribution and Zeta potential of the nanoemulsion were determined by the dynamic light scattering (DLS) method using the SZ-100Z2 device (Horiba, Japan). The nanoemulsions were diluted 100 times with distilled water for taking DLS spectra [8]. The ultraviolet-visible (UV - Vis) spectrum of nanoemulsion was taken using a UV-Vis S80 (Biochrom, UK).

3. RESULTS AND DISCUSSION

3.1. Pseudo-ternary phase diagram

Setting up a pseudo-ternary phase diagram is to find the suitable content range of components in a stable emulsion system. Figure 1 presents the pseudo-ternary phase diagram of SO, surfactant, and distilled water. The suitable content of SO, surfactant, and distilled water is from 9 - 32 %, 10 - 33 %, and 20 - 85 %, respectively.

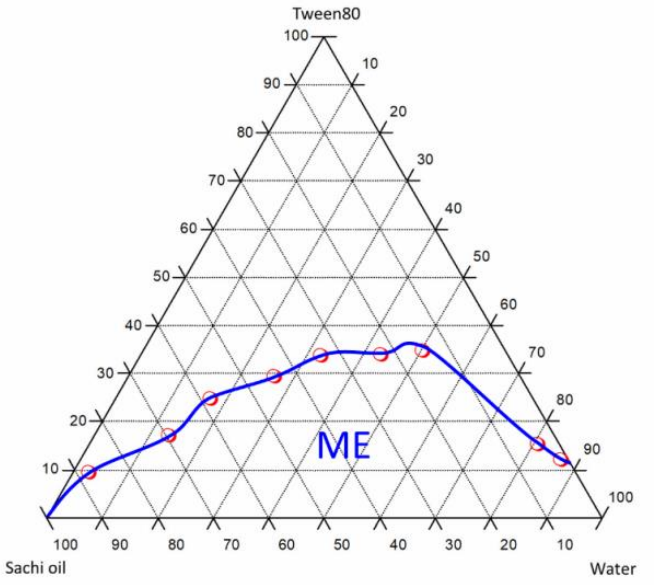

Figure 1. Pseudo-ternary phase diagram of SO, Tween80, and distilled water.

3.2. Experimental planning matrix and significance of the model

The experimental planning matrix of the emulsion process and the value of the objective function are presented in Table 2. The values are means of triplicate experiments. It can be seen that the values of the objective function of 15 experiments ranged from 60.93 ± 2.65 nm to 468.73 ± 11.67 nm. The component content has a strong effect on the objective function. The lowest value objective function was obtained at the center point conditions of SO of 250 µL, Tween 80 of 300 µL, and distilled water of 500 µL.

The significance of the quadratic model and coefficients of the equation reflecting the objective function was conducted by analysis of variance (ANOVA) and shown in Table 3.

Table 2. Experimental planning matrix for components in the nanoemulsion systems and obtained value of the objective function.

No.	Code Variable			Objective function – Droplet size (nm)
	A	B	C	
1	0	0	0	60.93 ± 2.65
2	-1	-1	0	468.73 ± 11.67
3	0	-1	1	356.93 ± 23.59
4	1	1	0	317.37 ± 27.70
5	-1	1	0	290.03 ± 25.19
6	0	0	0	94.77 ± 2.57
7	1	-1	0	97.07 ± 2.99
8	-1	0	-1	115.40 ± 1.45
9	0	1	1	216.60 ± 32.71
10	1	0	1	178.50 ± 6.28
11	0	1	-1	279.40 ± 29.65
12	-1	0	1	346.90 ± 28.69
13	0	-1	-1	87.97 ± 1.13
14	1	0	-1	179.33 ± 6.37
15	0	0	0	98.87 ± 3.07

Table 3. ANOVA analysis of objective function according to a quadratic model.

Source	Droplet size (nm)	
	F - value	p-value
Model	14.20	0.0047^{**}
A-A	15.46	0.0111^{*}
B-B	0.6594	0.4537^{NS}
C-C	14.64	0.0123^{*}
AB	24.43	0.0043^{**}
AC	8.28	0.0347^{*}
BC	16.89	0.0093^{**}
A^2	18.01	0.0081^{**}
B^2	32.27	0.0024^{**}
C^2	2.19	0.1994^{NS}
Lack of Fit	5.59	0.1554^{NS}
R^2		0.9624
Adjusted R^2		0.8946
Adeq-Precision		10.7031

***: $p < 0.01$; *: $p < 0.05$: Significant values; $^{NS}p > 0.05$: Not significant values*

The data in Table 3 indicated that the quadratic model is highly compatible with experiments with the Fisher standard (F-value) of 14.20 [15 - 18]. This model has a high reliability with a p-value of 0.0047 < 0.1 %. The suitability of the experiment with the quadratic model is also verified by the regression coefficient, R^2. The closer the R^2 value is to 1, the closer the experimental value is to the model's predicted value. As observed from data in Table 3, R^2 value of this model is 0.9624 (96.24 %), the adjusted R^2 value of this model is 0.8946 (89.46 %) and the Adeq-Precision value is 10.7031. The model has high compatibility with the experiment when both R^2 and Adj-R^2 values are greater than 0.8 and an Adeq-Precision is greater than 4 [16 - 18]. Additionally, the lack of fit p-value of the objective function is higher than 0.05 indicating that lack of fit is not meaningful. All of them confirmed that the quadratic model is the most appropriate fit for the experiment.

The compatibility of the quadratic model with the experiment can also be evaluated through the graphs of predicted and actual value and residuals versus runs models as shown in Figure 2. It can be seen a good correlation between experiment and theory due to the experimental points are concentrated in a straight diagonal form in the first graph and the distribution of experimental points is random within the range (- 4, 4) in the second graph in Figure 2.

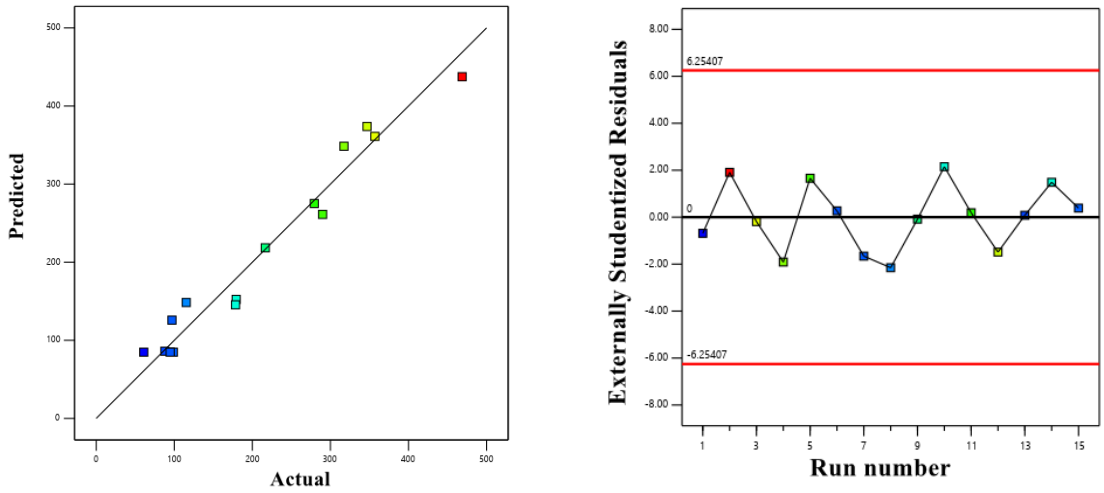

Figure 2. Graphs of the experimental and predicted graph, distribution of objective function.

According to that, the influence of linear effects (A, B, C) on the objective function is the largest, followed by the influence of double interaction effects (AB, AC, BC) and the influence of squared effects (A^2, B^2, C^2) is the least [16, 18]. From Table 3, the p-values for terms A, C, AB, AC, BC, A^2, and B^2 were lower than 0.05, indicating their significant impact when added to the quadratic model. There are two non-significant values of terms B and C^2 with a p-value higher than 0.05. These significant terms have remained in the models while the non-significant terms were removed. Therefore, the objective function model has been determined by a regression equation following the quadratic model:

Droplet size = 84.8567 - 56.0988 A + 54.6037 C + 99.75 AB – 58.0825 AC – 82.94 BC + 89.1245 A^2 + 119.318 B^2 (1)

From the regression equation (1), it can be seen a clear influence of technological factors on the objective function (droplet size). Among the three linear effects A, B, and C, factors A and C have a great influence on the objective function, in which, factor A shows a negative interaction effect while factor C shows a positive interaction effect on the objective function as the presence by their coefficients in the equation (1). The double interaction AB shows a positive interaction effect while the double interactions AC and BC show a negative interaction effect on the objective function corresponding to their coefficients in the equation (1). The squared effects A^2 and B^2 represent a positive interaction effect on the objective function corresponding to their coefficients in the equation (1). However, the squared effects have a very small effect on the objective function as mentioned above.

3.3. Optimization of the component of nanoemulsion

The ratio components of nanoemulsion need to be optimized so that the objective function reaches the smallest value. This is solved by the optimization using RSM and BBD with priority

levels from 1 to 5. In this problem, with the set goals, we choose the priority level for the objective function to be level 5.

Optimal results give us one solution corresponding to one set of optimal technology data. The optimal results are presented in Figure 3A. Under the conditions of technological parameters, the predicted value of the objective function, droplet size is of 56.714 (nm) (Figure 3A). The desirability of variables and objective function at the optimal conditions is shown in Figure 3B. The optimal volumes of SO, Tween 80, and distilled water are 266, 264, and 483 µL, corresponding to 26.26, 26.06, and 47.68 %, respectively.

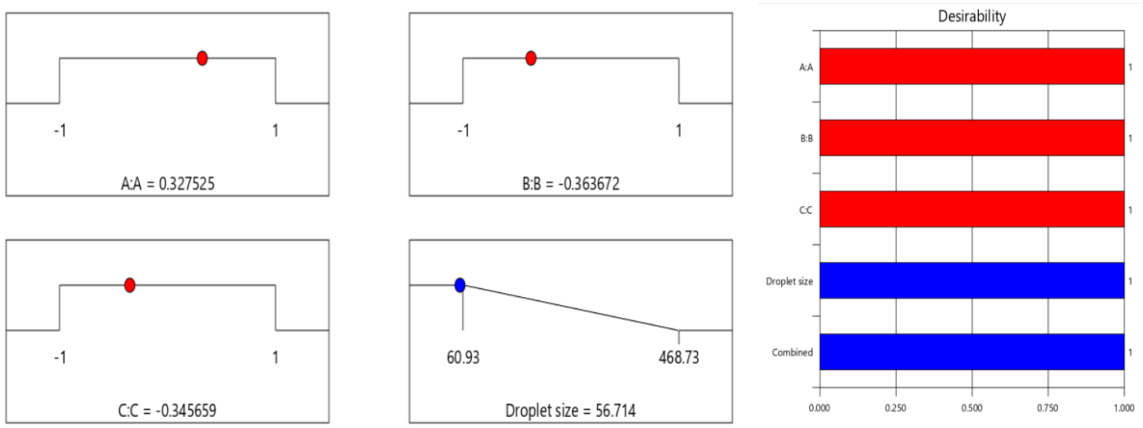

(A) (B)

Figure 3. Optimal conditions and predicted value of objective function (A) and desirability of variables and objective function (B).

The influence of pairs of technological factors expressed in the double interaction effect on the objective function is expressed through the response surfaces of droplet size of the nanoemulsion as shown in Figure 4. In each response surface, the dark blue area is the optimal area, where, the objective function values are in the smallest value region, and the light blue, green, and yellow areas represent regions with increasing objective function values. From Figure 4, it can be seen that the optimal area is the biggest.

3.4. Validation of optimization

Three validation trials of the nanoemulsion were prepared under the optimal conditions to determine the accuracy of the above design. Figure 5 presents the size distribution diagrams of the nanoemulsions prepared under the optimal conditions including 266 µL of SO, 264 µL of Tween 80, and 483 µL of distilled water. It can be seen that the emulsions have a nanometer size ranging from 35 to 110 nm, and the variation of trials is negligible. Table 4 displays the actual and predicted values of droplet size of the nanoemulsions. The values of the actual droplet size of the nanoemulsions are close to the predicted value, suggesting high suitability between the predicted model and experiments. From Table 4, the value of the polydispersity index (PI) is lower than 0.3. According to the report of Putri *et al.* for lipid-based carriers, the PI value lower than 0.3 is considered to be acceptable and indicates a homogenous distribution [19]. So, the nanoemulsions prepared under the optimal conditions in this study have a mid-range polydispersity.

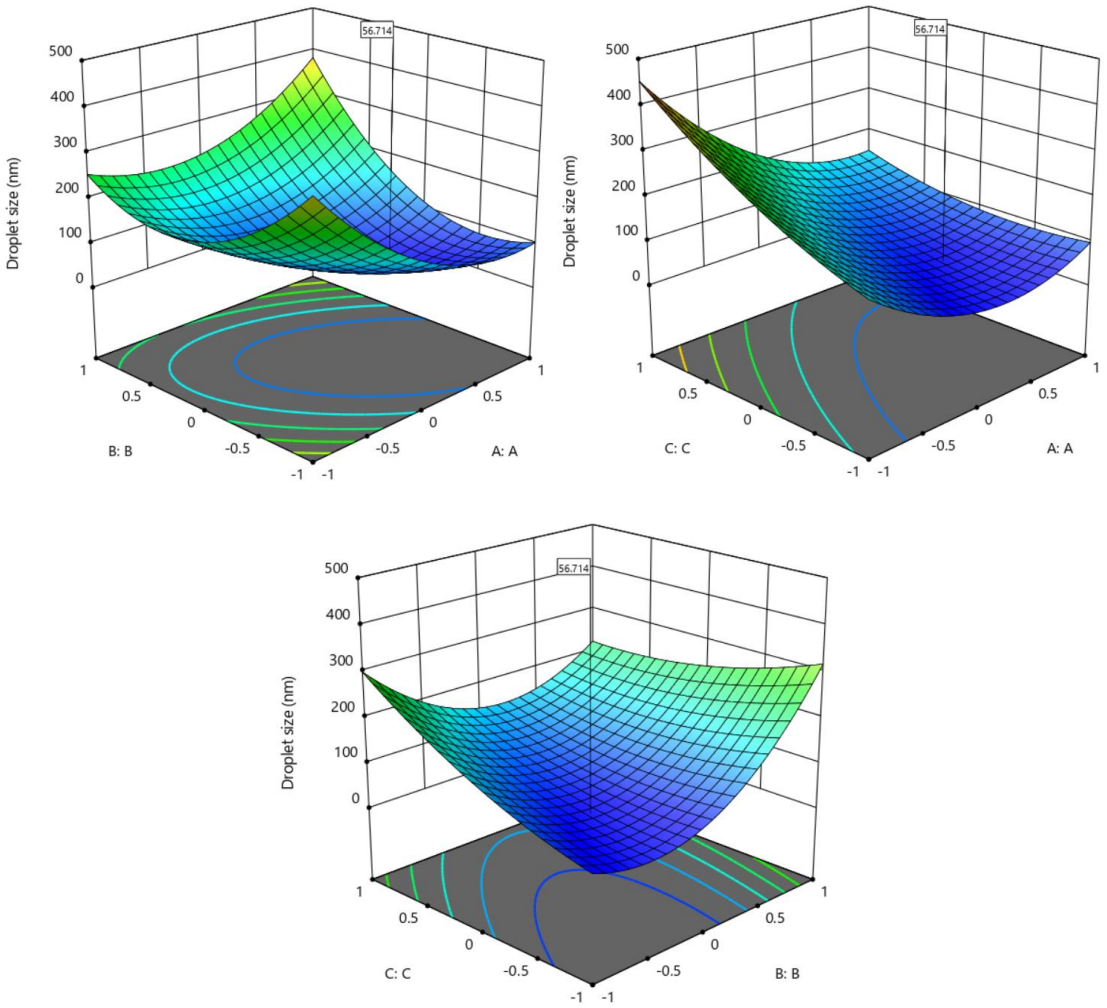

Figure 4. Surface response of droplet size of the nanoemulsion under the double interactions.

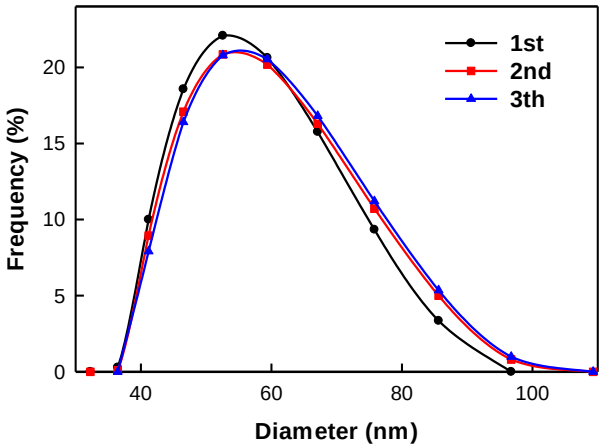

Figure 5. Size distribution diagrams of the nanoemulsions prepared under the optimal conditions.

Table 4. The droplet size of the nanoemulsion prepared under the optimal conditions

No.	Droplet size (nm)	PI	Predicted value of droplet size
1	56.3	0.305	56.714
2	59.3	0.241	
3	58.1	0.303	
Average	57.9 ± 1.5	0.283 ± 0.036	

3.5. Some characteristics of the nanoemulsion prepared under the optimal conditions

Zeta potential of the nanoemulsion prepared under the optimal conditions has been also evaluated by the DLS method. The result reveals that the surface of the nanoemulsion has a negative charge, - 25.2 mV. The high value of Zeta potential suggests that the nanoemulsion can disperse stably in the aqueous environment [20].

To evaluate the stability of the nanoemulsion in the aqueous environment, the average droplet size of the nanoemulsion was determined for samples with different diluting times. As seen from Table 5, the average droplet sizes of the sample when diluting 20 - 100 times are similar, indicating that the nanoemulsion has a high stability.

Table 5. Variation of the size distribution of the nanoemulsion when diluted with distilled water.

No.	Diluted times	Average droplet size (nm)	PI
1	20	56.4 ±1.7	0.193 ± 0.009
2	40	56.0 ±1.6	0.198 ± 0.007
3	80	55.0 ±0.8	0.223 ± 0.012
4	100	57.9 ± 1.5	0.283 ± 0.036

The UV-Vis spectra of the nanoemulsion that was diluted with distilled water at different ratios were demonstrated in Figure 6. The absorption peak at about the wavelength ranging from 200 - 300 nm was assigned to the polyunsaturated fatty acids in the nanoemulsion [21]. The absorbance intensity of the nanoemulsion when diluting 40 - 100 times is the same, suggesting that the nanoemulsion droplets are stable in aqueous environment. This result is in agreement with the size distribution result as aforementioned.

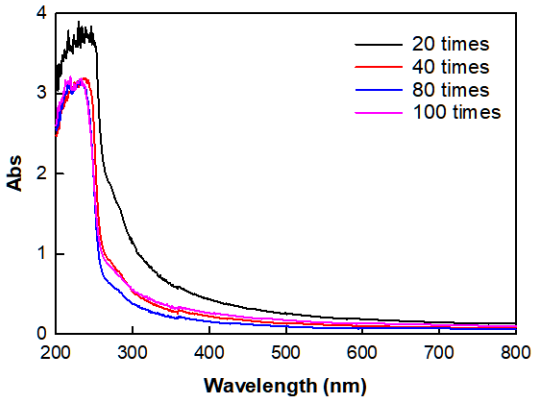

Figure 6. UV-Vis spectra of the nanoemulsion prepared under the optimal conditions.

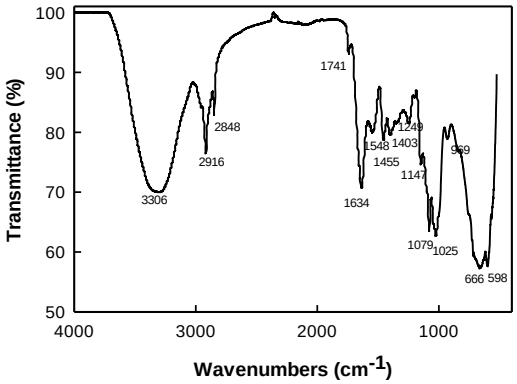

Figure 7. IR spectrum of the nanoemulsion prepared under the optimal conditions.

Figure 7 presents the IR spectrum of the nanoemulsion prepared under the optimal conditions. It can be seen some peaks are characterized by the vibrations of functional groups of SO and Tween 80. For instance, a peak at a wavenumber of 3306 cm^{-1} is assigned to the stretching vibration of O-H linkage, peaks at 2916 2848, 1455, and 1403 cm^{-1} are contributed to the stretching and bending vibrations of the C-H bond, peak at 1741 cm^{-1} is found by the stretching vibration of C=O bond, peak at 1634 cm^{-1} is corresponded to the stretching vibration of C=C bond, peak at 1548 cm^{-1} is attributed to the bending vibration of O-H linkage, peaks at 1025-1249 cm^{-1} is due to stretching vibration of C-O and C-C linkages [7, 8, 10].

The stereo microscopy (SM) images of the nanoemulsion prepared under the optimal conditions are displayed in Figure 8. The sample was diluted 20 times and 100 times with distilled water. The emulsion droplets are spherical and they do not agglomerate to each other. This result is evidence for the dispersibility of the nanoemulsion in the aqueous environment.

The obtained results indicated that the nanoemulsion from SO, Tween 80, distilled water at the optimal conditions is highly stable and of small size, thus, they are suitable for loading bioactive agents, such as vitamins or nutraceuticals. However, to open the application of the nanoemulsion in practice, it should be evaluated the bioactivities and layer separation of this nanoemulsion system.

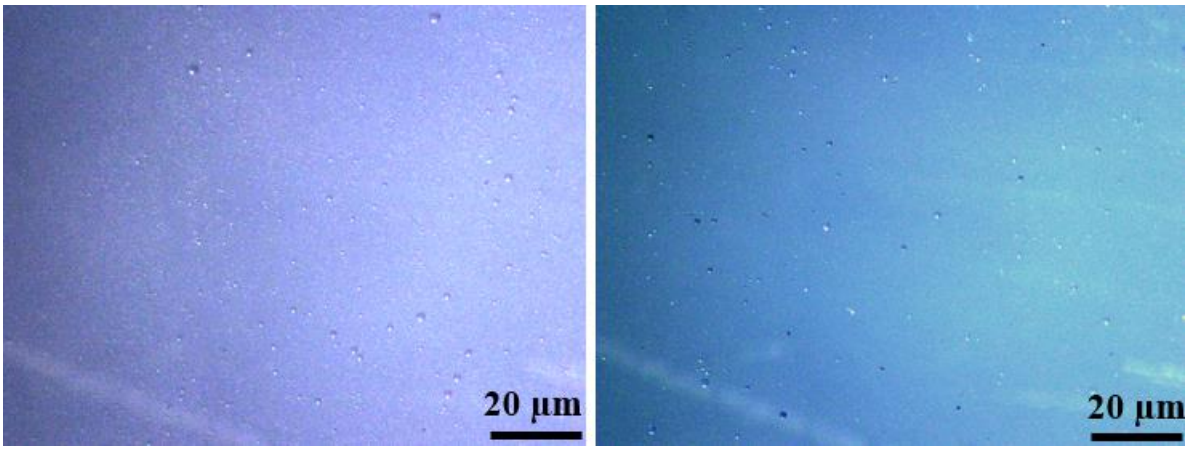

Figure 8. SM images of the nanoemulsion prepared under the optimal conditions with diluting 20 times (left) and diluting 100 times (right).

4. CONCLUSIONS

In conclusion, the nanoemulsions based on Sachi seed oil (SO), Tween 80, and distilled water have been prepared successfully. The optimization by response surface method found the optimal contents of these components in the nanoemulsion. The optimal contents of SO, Tween 80, and distilled water are 26.26, 26.06 and 47.68 %, respectively. Under the optimal conditions, the nanoemulsion had a high stability with an average droplet size of 57.9 ± 1.5 nm and a negative surface charge of - 25.2 mV. The nanoemulsion droplets were stable in the aqueous solution and the droplet size mostly unchanged by diluting. They are spherical and separated in the aqueous solution. This obtained result indicated that the nanoemulsion from SO, Tween 80, and distilled water is promising for application in functional foods and health care.

Acknowledgment. This research is funded by the Vietnam Academy of Science and Technology under grant number UDSXTN.06/23-24.

CRediT authorship contribution statement. Dam Xuan Thang: Methodology, Formal analysis. Cung Dinh Duc, Nguyen Ngoc Quynh: Investigation. Pham Thi Tham: Supervision. Thai Hoang: Writing-Reviewing and Editing. Nguyen Phi Hung: Formal analysis. Nguyen Thuy Chinh: Supervision, Writing-original draft preparation, Funding acquisition.

Declaration of competing interest. The authors declare that they have no known competing financial interests or personal relationships that could have appeared to influence the work reported in this paper.

REFERENCES

1. Nur A.R. M. R. and Lai K. L. - Sacha Inchi (*Plukenetia Volubilis* L.): recent insight on phytochemistry, pharmacology, organoleptic, safety and toxicity perspectives, Heliyon **8** (9) (2022) e10572. https://doi.org/10.1016%2Fj.heliyon.2022.e10572.
2. Alexandra V., Frank L. R. O., Adriana V. O., Dayana B. R., Ana M. M. and Fernando R. E. - Sacha Inchi Seed (*Plukenetia volubilis* L.) Oil: Terpenoids, in: Shagufta P. and Areej M. A. T. (Eds), Terpenes and Terpenoids - Recent Advances, Intechopen Limited Publishing, London, 2021. DOI: 10.5772/intechopen.96690.
3. Ankit G., Beenu T., Manvesh K. S., Vivek S. - Sacha inchi (*Plukenetia volubilis* L.): An emerging source of nutrients, omega-3 fatty acid and phytochemicals, Food Chem. **373** (B) (2022) 131459. https://doi.org/10.1016/j.foodchem.2021.131459.
4. Norhazlindah M. F., Jahurul M. H. A., Norliza M., Shihabul A., Shahidul I., Nyam K. L., Zaidul I. S. M. - Techniques for extraction, characterization, and application of oil from sacha inchi (*Plukenetia volubilis* L.) seed: a review, J. Food Meas. Charact. **17** (2023) 904–915. https://doi.org/10.1007/s11694-022-01663-0.
5. Sunan W., Fan Z., Yukio K. - Sacha inchi (*Plukenetia volubilis* L.): Nutritional composition, biological activity, and uses, Food Chem. **265** (2018) 316-328. https://doi.org/10.1016/j.foodchem.2018.05.055.
6. Cang M. H., Chinh N. D., Nhan N. P. T., Giang B. L. - Physico-chemical properties of sacha inchi (*Plukenetia volubilis* L.) seed oil from Vietnam, Asian J. Chem. **32** (2020) 335-338. https://doi.org/10.14233/ajchem.2020.22233.
7. Xiaoqiu S., Jinyu W., Shuaitao L., Yifei W. - Formation of sacha inchi oil microemulsion systems: effects of non-ionic surfactants, short-chain alcohols, straight-chain esters and essential oils, J. Sci. Food Agric. **102** (9) (2022) 3572-3580. https://doi.org/10.1002/jsfa.11703.
8. Suraj K. M., Atmaram P. P. - Preparation, optimization and preliminary pharmacokinetic study of curcumin encapsulated turmeric oil microemulsion in zebra fish, Eur. J. Pharm. Sci. **155** (2020) 105539. https://doi.org/10.1016/j.ejps.2020.105539.
9. Huy N. M., Hien T. T. B., Thoai N. D. - Preparation and formulation of self-microemulsifying drug delivery system (SMEDDS) containing diclofenac, J. Military Pharm. Med. **5** (2021) 5-16.
10. Yeon-Ji J., Heike P. K., Ulrike S. van der S. - Collagen peptide-loaded W1/O single emulsions and W1/O/W2 double emulsions: influence of collagen peptide and salt concentration, dispersed phase fraction and type of hydrophilic emulsifier on droplet stability and encapsulation efficiency, Food Funct. **10** (2019) 3312-3323, https://doi.org/10.1039/C8FO02467G.
11. Jaiswal M., Dudhe R., Sharma P. K. - Nanoemulsion: an advanced mode of drug delivery system, 3 Biotech. **5** (2) (2015) 123-127. https://doi.org/10.1007%2Fs13205-014-0214-0.

12. Lei J., Gao Y., Hou X., Sheng Z., Zhang C., Du F. - A simple and effective strategy to enhance the stability and solid-liquid interfacial interaction of an emulsion by the interfacial dilational rheological properties, Soft Matter. **16** (24) (2020) 5650-5658. https://doi.org/10.1039/D0SM00638F.
13. Mundada V., Patel M., Sawant K. - Submicron emulsions and their applications in oral delivery, Crit Rev Ther Drug Carrier Syst. **33** (3) (2016) 265-308. https://doi.org/10.1615/critrevtherdrugcarriersyst.2016017218.
14. Kiattiphumi S., Ampa J. - Determination of hydrophilic–lipophilic balance value and emulsion properties of sacha inchi oil, Asian Pac. J. Trop. Biomed. **7** (12) (2017) 1092-1096. https://doi.org/10.1016/j.apjtb.2017.10.011.
15. Noordin M. Y., Venkatesh V. C., Sharif S., Elting S., Abdullah A. - Application of response surface methodology in describing the performance of coated carbide tools when turning AISI 1045 steel, J. Mater. Process Technol. **145** (1) (2004) 46-58. https://doi.org/10.1016/S0924-0136(03)00861-6.
16. Sarah W., Shaobo D., Jun Z., Muhammad A. B., Forrest I. - Optimization of a novel liquid-phase plasma discharge process for continuous production of biodiesel, J. Clean Prod. **228** (2019) 405-417. https://doi.org/10.1016/j.jclepro.2019.04.311.
17. Verma R., Kumar M. - Development and optimization of methotrexate encapsulated polymeric nanocarrier by ionic gelation method and its evaluations, ChemistrySelect **7** (48) (2022) e202203698. https://doi.org/10.1002/slct.202203698.
18. Yusuff A. S., Ishola N. B., and Gbadamosi A.O. - Artificial intelligence techniques and response surface methodology for the optimization of methyl ester sulfonate synthesis from used cooking oil by sulfonation, ACS Omega **8** (22) (2023) 19287–19301. https://doi.org/10.1021/acsomega.2c08117.
19. Putri D. C., Dwiastuti R., Marchaban M., Nugroho A. K. - Optimization of mixing temperature and sonication duration in liposome preparation, J. Pharm. Sci. Commun. **14** (2017) 79–85. doi: 10.24071/jpsc.142728.
20. Vallar S., Houivet D., El Fallah J., Kervadec D., Haussonne J. M. - Oxide slurries stability and powders dispersion: optimization with zeta potential and rheological measurements, J. Eur. Ceram. Soc. **19** (6–7) (1999) 1017-1021. https://doi.org/10.1016/S0955-2219(98)00365-3.
21. Ajay K. S., Anjali, Neelima V., Suruchi P., Kiran Y. V., Sanjeev K. M. - Optimizing a detection method for estimating polyunsaturated fatty acid in human milk based on colorimetric sensors, Mater. Sci. Energy Technol. **2** (3) (2019) 624-628. https://doi.org/10.1016/j.mset.2019.07.001.